Title: Distinct neural mechanisms and temporal constraints govern a cascade of audiotactile interactions

Abbreviated title: Audiotactile asynchronies elicit distinct effects

Johanna M. Zumer[1,2,3], Thomas P. White[1,2], Uta Noppeney[1,2,3]

[1]School of Psychology, University of Birmingham, Birmingham, B15 2TT, United Kingdom

[2]Centre for Computational Neuroscience and Cognitive Robotics, University of Birmingham, Birmingham, B15 2TT, United Kingdom

[3]Centre for Human Brain Health, University of Birmingham, Birmingham, B15 2TT, United Kingdom

Corresponding Author: Johanna Zumer, School of Psychology, University of Birmingham, Birmingham, B15 2TT, United Kingdom; johanna.zumer@gmail.com

Number of pages: 36

Number of figures: 6

Number of words in Abstract: 250

Number of words in Introduction: 648

Number of words in Discussion: 1477

Conflict of Interest: The authors declare no competing financial interests.

Acknowledgements: FP7 ERC Starting Grant multsens (U.N.) and FP7 Marie Curie IntraEuropean Fellowship ISMINO (J.M.Z. and U.N.). We thank Christoph Braun and Elisa Leonardelli for assistance with the tactile device and Máté Aller for assistance with EEG and stimulus setup.

Abstract

Synchrony is a crucial cue indicating whether sensory signals are caused by single or independent sources. In order to be integrated and produce multisensory behavioural benefits, signals must co-occur within a temporal integration window (TIW). Yet, the underlying neural determinants and mechanisms of integration across asynchronies remain unclear. This psychophysics and electroencephalography study investigated the temporal constraints of behavioural response facilitation and neural interactions for evoked response potentials (ERP), inter-trial coherence (ITC), and time-frequency (TF) power. Participants were presented with noise bursts, 'taps to the face', and their audiotactile (AT) combinations at seven asynchronies: 0, ±20, ±70, and ±500 ms. Behaviourally we observed an inverted U-shape function for AT response facilitation, which was maximal for synchronous AT stimulation and declined within a ≤70 ms TIW. For ERPs, we observed AT interactions at 110 ms for near-synchronous stimuli within a ≤20 ms TIW and at 400 ms within a ≤70 ms TIW consistent with behavioural response facilitation. By contrast, AT interactions for theta ITC and ERPs at 200 ms post-stimulus were selective for ±70 ms asynchrony, potentially mediated via phase resetting. Finally, interactions for induced theta power and alpha/beta power rebound emerged at 800-1100 ms across several asynchronies including even 500 ms auditory leading asynchrony. In sum, we observed neural interactions that were confined to or extending beyond the behavioural TIW or specific for ±70 ms asynchrony. This diversity of temporal profiles and constraints demonstrates that multisensory integration unfolds in a cascade of interactions that are governed by distinct neural mechanisms.

Significance Statement:

Integrating information across audition and touch is critical for effective interactions with our environment. We are faster to swat a mosquito when we perceive a prick on the skin together with hearing the mosquito's buzzing. Importantly, we should integrate signals only when they co-occur within a temporal integration window (TIW) and are hence likely to originate from a common source. This psychophysics/electroencephalography study unravels a multitude of neural interactions governed by different temporal constraints: interactions were confined to a TIW for ERPs, specific for one particular asynchrony for inter-trial coherence, and extending beyond the behavioural TIW for induced low frequency power. This diversity of temporal profiles demonstrates that distinct neural mechanisms mediate a cascade of multisensory integration processes.

Introduction

Imagine sitting outside on a summer evening. Suddenly you hear a buzz and then feel a prick to your skin, as the mosquito lands. You are faster to swat it away because you first heard it coming. This faster detection of a multisensory event is known as the redundant target effect (RTE) (Miller, 1982, Diederich and Colonius, 2004, Sperdin et al., 2009) and illustrates the enormous benefits of multisensory integration.

Importantly, we should integrate signals only if they arise from a common source but segregate them otherwise. Synchrony is a critical cue for determining whether two signals come from a common source. Multisensory need to co-occur within a certain tolerance of asynchrony, termed a temporal integration window (TIW) (Diederich and Colonius, 2004). In particular, the RTE typically follows an inverted U-shape function (Blurton et al., 2015) that is maximal for (near)-synchronous signals and tapers off with increasing asynchrony thereby moulding the TIW.

Likewise, observers' perceived synchrony, the emergence of cross-modal biases, and perceptual illusions follow a similar inverted U-shape function with its exact shape varying across different behavioural measures and task-contexts (van Wassenhove et al., 2007, Megevand et al., 2013, Berger and Ehrsson, 2014, Donohue et al., 2015).

At the neural level, multisensory influences have been identified in terms of response enhancements and suppressions, super-additive and sub-additive interactions (Meredith and Stein, 1983, Stanford et al., 2005, Werner and Noppeney, 2010b), shortened neural response latencies (Rowland and Stein, 2007) and altered neural representations (Fetsch et al., 2011, Rohe and Noppeney, 2015, 2016). Evidence from neuroimaging, neurophysiology, and neuroanatomy has shown that multisensory influences emerge at early and late stages of neural processing (Foxe et al., 2000, Lutkenhoner et al., 2002, Murray et al., 2005, Senkowski et al., 2008, Sperdin et al., 2009, Stekelenburg and Vroomen, 2009, Mercier et al., 2013, Mercier et al., 2015) nearly ubiquitously in neocortex (Schroeder and Foxe, 2002, Ghazanfar and Schroeder, 2006, Lakatos et al., 2007, Werner and Noppeney, 2010a, Ibrahim et al., 2016, Atilgan et al., 2018). They arise already at the primary cortical level and increase progressively across the sensory processing hierarchy (Foxe and Schroeder, 2005, Bizley et al., 2007, Kayser et al., 2007, Dahl et al., 2009). This multi-stage and multi-site account of multisensory interplay raises the question of whether the myriad of multisensory influences is governed by similar neural mechanisms and temporal constraints. Further, how do those neural effects relate to the TIW defined by behavioural indices? Given previous unisensory research showing an increase in the TIW along the sensory processing hierarchy (Hasson et al., 2008, Kiebel et al., 2008), one may for instance hypothesise that early multisensory interactions are confined to narrower temporal integration windows than those occurring at later stages in higher order association cortices (Werner and Noppeney, 2011).

Moreover, recent neurophysiological studies suggest that multisensory interactions depend on the phase of ongoing neural oscillations and/or rely on mechanisms of phase resetting. For instance, Lakatos et al. (2007) showed that a tactile signal can reset the phase of ongoing oscillations in auditory cortices, but only for specific asynchronies.

The current study aims to define the temporal constraints of multisensory interactions that can be observed for evoked response potentials (ERP), inter-trial coherence (ITC), and induced power responses and relate those to the TIW derived from behavioural response facilitation. Participants were presented with brief airpuff noise bursts, 'taps to the face' and their audiotactile (AT) combinations at seven levels of asynchrony: 0, ±20, ±70, and ±500 ms. In the psychophysics study observers were instructed to respond to all A, T, and AT events in a redundant target paradigm; in the EEG study a passive stimulation design was used to avoid response confounds. We then identified multisensory influences in terms of multisensory interactions (i.e. AT + No stimulation ≠ A + T) separately for each AT asynchrony level for ERPs, ITC, and induced power responses and characterised their topography across post-stimulus time.

Materials and Methods

Participants. Twenty-five healthy, adult participants with no neurological disorder were recruited from the local university population (students as well as members of the general public) (N=25, 12 female and 13 male; aged between 18-35 years old). One participant was excluded due to an abnormal finding in the structural MRI. Two participants were excluded from the behavioural analysis, because data were not collected for all conditions. Two different participants were excluded from the EEG analysis, because insufficient EEG data were collected.

As a result we included 22 participants in both the behavioural and EEG analysis. They gave written informed consent and were compensated either with cash or course credit. Ethical approval for the study was given by the University of Birmingham Science, Technology, Engineering, and Mathematics Review Committee with approval number ERN_11-0429AP22B.

Stimulation. Tactile stimulation consisted of a touch to the left side of the face with 200 ms duration. Tactile stimulation to the face was used as an ecologically valid stimulus that requires a rapid response in everyday life. We also chose stimulation to the face (in contrast to hands), as this body location does not require additional processing of being potentially crossed relative to body position, thus potentially amenable to a quicker and more automatic route. The auditory association areas that receive feed-forward (layer 4) input from somatosensory stimulation appear to be optimally stimulated by cutaneous stimulation of the head and neck (Fu et al., 2003). The left side was chosen based on previous findings that MSI is enhanced with left-side stimulation and right hemisphere involvement (Giard and Peronnet, 1999, Downar et al., 2000, Molholm et al., 2002, Hoefer et al., 2013). The part of the face touched was on/near the border between the maxillary (V2) and mandibular (V3) divisions of the trigeminal cranial nerve. A fibre optic cable (part of a fibre optic system: Keyence series FS-N, Neu-Isenburg, Germany) was attached to a Lego pneumatic cylinder and driven to move by pressurised air. The tip of this cable (3 mm diameter) was positioned near the face using a flexible plastic snap-together 'goose-neck' pipe that was attached to an adjustable stand. The air pressure changes were controlled by a microcontroller connected via USB to the stimulus computer; communication to the microcontroller was sent via serial port commands in MATLAB (Mathworks, Inc.). The duration of the open valve (i.e. when the diode was extended forward to touch the skin) was set to 200 ms. The fibre optic cable contained a dual fibre: one fibre projected light and the other

was a photodiode that detected the light reflectance; from this, the reflectance dynamics confirmed the exact timing of the touch to the skin. This tactile apparatus was very similar to that used by Leonardelli et al. (2015). After the experiment, subjects were queried as to whether they could hear the tactile device moving prior to it touching them and none reported that they could.

The auditory stimulus (target) was an airpuff noise of 200 ms duration. The volume of the target was well above threshold for detection but not painfully loud; the volume was stronger on the left channel than on the right (interaural intensity difference) to create the perception of coming from the left. A constant background noise of a recording of a magnetic resonance imaging (MRI) echo-planar imaging sequence (obtained from http://cubricmri.blogspot.co.uk/2012/08/scanner-sounds.html) was played to help mask external noises including those made by the tactile stimulator and for comparison with potential future functional MRI studies. The volume of the background noise, equally loud in both ears, was played at a level comfortable to participants and such that the tactile noises could not be heard. All sounds were presented via E-A-RTone earphone (10 Ohm; E-A-R Auditory Systems) with plastic tube connection (length = 75 cm) to foam ear insert (E-A-RLink size 3A), which also acted as an earplug against external sounds.

Experimental design. Participants took part in one psychophysics and one EEG session on separate days (typically 4-6 days gap). The experimental design and stimuli were identical across the two sessions. In the psychophysics session participants responded to the first stimulus in a trial irrespective of sensory modality, as fast as possible via a single key board button (i.e. redundant target paradigm). In the EEG session, participants passively perceived the stimuli

without an explicit response in order to avoid motor confounds and allow for comparison with sleep, non-responsive patients, etc.

In each session, participants were presented with the following trial types: no stimulus (or null) condition (N), tactile alone (T), auditory alone (A), and seven audiotactile (AT) conditions varying in asynchrony (-500 ms, -70 ms, -20 ms, 0 ms, 20 ms, 70 ms, 500 ms) where a 'negative' asynchrony refers to A-leading-T (Fig. 1a). The audiotactile conditions are referred to by the following abbreviations: AT500, AT70, AT20, AT0, TA20, TA70, TA500, respectively. These asynchronies were chosen to fall either within the behaviourally-defined temporal integration window (TIW) (≤70 ms) based on previous studies (e.g. (Navarra et al., 2007, Harrar and Harris, 2008, Nishi et al., 2014)) or outside the TIW (± 500 ms). Ten different trial types were presented, interleaved randomly with an inter-trial interval uniformly distributed between 2.0 – 3.5 s, including both unisensory and audiotactile conditions with varying asynchronies between the sensory stimuli. Each trial type was presented 100 times in each session. Trials were presented in blocks of 250 trials (roughly 11.75 minutes) over four blocks separated by short breaks. In the EEG session (performed about 1 hour before bedtime) we occasionally shortened the blocks, but still presented 1000 trials in total. In the psychophysics session the AT500 and TA500 conditions were not collected for two participants; thus for behavioural results, only the data from the remaining twenty-two participants are included (after exclusion also of one participant for the afore-mentioned structural MRI abnormality).

Participants kept their eyes closed to obliterate any visual input throughout the experiment. They were seated comfortably with their head stabilised in an adjustable chin rest and were requested to hold their head as still as possible (to promote spatial and temporal consistency of the tactile stimulation over trials).

184 *EEG recording.* EEG data were recorded with a 64 channel BrainProducts MR-compatible
185 cap at 1000 Hz sampling rate, with 63 of the electrodes on the scalp. For all but the first three
186 participants, two additional bipolar electrodes were placed on the face to record horizontal EOG
187 and vertical EOG. For 17 participants, the 64th cap electrode was placed on the participants' back
188 for recording ECG. For the other 8 participants, the 64th electrode was instead placed on the
189 right (unstimulated) cheek for assistance as EOG/EMG. Signals were digitised at 5000 Hz with
190 an anti-aliasing filter of 1000 Hz, then down-sampled to 1000 Hz with a high-pass filter of 0.1
191 Hz and low-pass filter of 250 Hz. Electrode impedances were kept below 25 kOhm. Triggers
192 from the stimulus-control computer were sent via LabJack to the EEG acquisition computer.
193 *Tactile stimulation output*: The time course of light reflectance was assessed for each tactile
194 trial to ensure that i. the tactile device actually touched the skin and ii. to determine the touch
195 onset time (1000 Hz sampling rate). After computing the actual onset of the touch from the light
196 reflectance data, subsequently the exact multisensory onset asynchrony was computed for all
197 multisensory trials. Those that deviated by more than ± 5 ms from the desired asynchrony were
198 discarded. This resulted in 16.8% (± 1.1%) and 16.4% (± 1.2%) of trials rejected for the
199 behavioural and EEG data, respectively (N=24, after excluding the participant with structural
200 MRI abnormality).
201 *Behavioural analysis.* After exclusion of trials where touch was not applied or outside the
202 desired asynchrony, sensory trials were additionally discarded with no response or with response
203 times (RT) faster than 100 ms or slower than 1 s (occurring in total for an average of 2.7±1.1%
204 of trials across conditions). The median RT within a condition for each participant was
205 computed.

For each participant the *redundant target effect* (Hershenson, 1962) was computed for each participant by subtracting the median RT of the AT condition at a particular level of asynchrony from the fastest A or T condition with the onset of each unisensory condition adjusted for the particular asynchrony (e.g. $RT_{AT20} - \min(RT_T + 20\text{ ms}, RT_A)$. Using a one-sample two-sided t-test we assessed whether the redundant target effect differed significantly from zero across participants.

EEG analysis: sleep staging. To ensure that only EEG data was used in which participants were awake, given the passive stimulation design with eyes closed and the evening acquisition, standard sleep scoring was performed using American Academy of Sleep medicine (AASM) 2007 criteria in the FASST open-source software (http://www.montefiore.ulg.ac.be/~phillips/FASST.html) (Leclercq et al., 2011) and custom code in MATLAB. Data were segmented into 30 s chunks and referenced to linked-mastoids. Sleep stages were assessed by two of the authors (J.M.Z. and T.P.W.) independently with a correspondence of 88%. Differences were discussed and a consensus reached (with correspondence of the consensus to each assessor's scores at 93% and 94%). Any 30 s chunk that was not scored as 'awake' was excluded from further analysis. If an individual participant had fewer than 55 trials per condition remaining in the awake stage (prior to artefact rejection), the participant was fully excluded. Two participants were excluded for this reason.

EEG analysis: preprocessing: All subsequent EEG data processing (after sleep staging) was performed using the open-source toolbox FieldTrip (Oostenveld et al., 2011) (www.fieldtriptoolbox.org) and custom code in MATLAB. Eye movement artefacts were automatically detected using three re-referenced bipolar pairs ('F7-F8', 'Fp2-FT9', and 'Fp1-FT10') and the VEOG if available. These channels' data were band-pass filtered (1-16 Hz;

Butterworth, order 3) and transformed to z-values. The exclusion threshold was set at a z-value of 6 and trials containing these artefacts were excluded. EEG data were re-referenced to the average reference, high-pass filtered (0.2 Hz), band-stop filtered around the line noise and its harmonics (49-51 Hz, 99-101 Hz, and 149-151 Hz), and epoched for each trial. Trials were locked to the onset of the tactile stimulus for tactile and all multisensory conditions and to the auditory or null trigger for A and N conditions, respectively. Initially, the epoch length was from -1.5 s to 2.3 s. Then A trials were shifted ± 0.5, 0.07, 0.02, or 0 s before being added to a T trial, to create the appropriate A+T combination to contrast with AT trials, hence resulting in variable lengths of pre-stimulus and post-stimulus window lengths, depending on the AT asynchrony.

EEG analysis: multisensory contrast. Multisensory integration in the EEG data was identified in terms of AT interaction, i.e. the sum of unisensory (A+T) contrasted to the audiotactile plus null (AT+N). It is critical to add the null condition (to the multisensory) to account for non-specific effects in a trial such as expectancy of stimulation as well as random noise. The sum of unisensory (A+T) trials was computed for each AT asynchrony level such that the onsets of the auditory and tactile stimuli were exactly aligned to the trials of the AT condition (i.e. we also accounted for the jitter of tactile onsets, see above). Trials from each condition were randomly sub-selected to ensure an equal number of trials per each of the four conditions in a given contrast (A, T, AT, and N). To correct for multiple comparison (over channels, time, and, where applicable, frequency) we performed cluster-based permutation tests for dependent (i.e. paired) samples, with the sum of the t values (i.e. max sum) across a cluster as cluster-level statistic and a cluster detected at an auxiliary uncorrected alpha threshold of 0.05.

EEG analysis: multisensory effects on ERP, inter-trial coherence, and time-frequency power. For the evoked response potential (ERP) analysis, EEG data were low-pass filtered (40 Hz). The

252 average over trials within a participant was computed for the combination of conditions A+T and
253 AT+N separately. We assessed the AT interaction separately for each asynchrony level within a
254 500 ms time window, beginning at the onset of the second stimulus.

255 For time-frequency analysis, EEG data were Fourier transformed with separate parameters for
256 lower (4-30 Hz) and higher (30-80 Hz) frequencies. Sliding time windows of length equal to
257 four cycles (low frequencies) or 200 ms (high frequencies) at a given frequency in steps of 2 Hz
258 (low frequencies) or 5 Hz (high frequencies), after application of a Hanning taper (low
259 frequencies) or multitaper with +/- 7 Hz smoothing (high frequencies). The complex values
260 were kept for separate analysis of the inter-trial coherence (ITC) (also referred to as phase-
261 locking factor or phase-consistency index) and the time-frequency (TF) power magnitude. Note
262 that the sum of trials of different condition types (i.e. A+T and AT+N) was computed prior to
263 Fourier transformation so that any cancellation due to phase differences would occur prior to
264 obtaining the Fourier complex value (see Senkowski et al. (2007)). The ITC was computed for
265 each condition and subject as the absolute value of the sum of the complex values over trials. We
266 assessed the AT interactions for ITC and TF power separately for 'low frequency' and 'high
267 frequency' and for each asynchrony level, within a 1200 ms time window beginning at the onset
268 of the second stimulus and extending to include the low frequency (e.g. alpha and beta)
269 desynchronization / rebound effects.

270

271 **Results**

272 For the psychophysics study we report the redundant target effect as a behavioural index of
273 audiotactile integration for each asynchrony level. For the EEG data we report the multisensory
274 interactions (AT+N $\neq$ A+T) for ERPs, inter-trial coherence (ITC), and time-frequency (TF)

power. Both behavioural and neural indices of multisensory integration were identified separately for each of the seven levels of AT asynchrony: 0, ±20, ±70, and ±500 ms (Figure 1a). This allows us to investigate if the integration indices were i. limited to temporal integration windows, ii. selective for specific asynchronies, or iii. symmetric for A-leading vs. lagging asynchronies.

Behavioural results: reaction time facilitation tapered by TIW

As expected, we observed significantly faster (Figure 2 for p-values and t-values) response times for the AT relative to the fastest unisensory condition (i.e. *redundant target effect*) for asynchronies within a ≤ 70 ms window of integration (Figure 1b). Specifically, the RTEs (across subjects mean ± SEM) for the different asynchrony levels were: AT70 = 35 ms ± 6 ms, AT20= 38ms ± 5 ms, AT0 = 35ms ± 4 ms, TA20 = 33ms ± 4 ms, and TA70 = 24ms ± 4 ms. Surprisingly, we observed significantly slower response times for the AT500 relative to the unisensory auditory condition, i.e. a negative redundant target effect (across subjects' mean ± SEM) = -16ms ± 4 ms. In summary, our psychophysics study revealed that audiotactile interactions within a 70 ms temporal integration window (TIW) facilitate stimulus processing and response selection leading to faster response times.

Audiotactile interactions for ERPs: limited to a TIW

Figure 1C shows the ERPs for the A, T, AT and N conditions. Both tactile-alone (pink) and auditory-alone (green) stimulation evoked a characteristic N100 followed by a P200, while the null condition is a flat baseline. The tactile and auditory stimulation together generate the AT evoked potentials across the different asynchrony levels (Figure 1C, black). While the influences

of both the tactile and auditory evoked responses are clearly visible in the AT responses, we can also observe small deviations from the unisensory responses. In the following, we investigate whether the AT+N responses deviate significantly from the sum of the A and T responses (i.e. the AT interaction).

Figure 3 shows the ERPs for the sum over A+T (dark blue), sum over AT + N (light blue), and the difference (A+T) – (AT + N), i.e. the audiotactile interaction effects across different asynchrony levels. For ERPs we observed three AT interaction effects that differed in their expression across levels of AT asynchrony (for significance of the test results, please see Figure 2).

The first AT interaction effect arose early, at about 100 ms post-stimulus, with a central topography and was significant only for the synchronous condition (Figure 3, AT0 row). Specifically, a modulation, during and after the N100 (70-170 ms), was found in both central and posterior sensors, with the A+T greater than the AT+N during this time. We note that a trend for this spatiotemporal effect was also observed for the AT20 condition.

The second AT interaction effect, where A+T was more negative than the AT+N, arose later at about 370-400 ms mainly over posterior electrodes for AT asynchrony conditions within a $\leq$ 20 ms temporal integration window (Figures 2, AT20, AT0, and TA20 rows). Even though this AT interaction effect was significant only for AT20 and TA20, we observed a qualitatively similar pattern for the synchronous AT0 condition.

The third AT interaction effect emerged at about 200 ms after the second stimulus (latency range: 140-220 ms), was most pronounced over frontocentral electrodes, and was selective for the asynchrony of ±70 ms (Figure 3, AT70 and TA70 rows). This AT interaction modulated the

shape and magnitude of the P200: the P200 occurred earlier and was reduced in amplitude for the AT+N relative to A+T.

In summary, we observed three distinct AT interaction effects for ERPs that were expressed at different AT asynchronies. Nevertheless, all AT interaction effects arose within the behavioural ≤ 70 ms TIW, while no significant AT interactions were found for the AT500 or TA500 conditions.

Audiotactile interactions for ITC: selective for ±70 ms asynchronies

Figure 4 shows the ITC for the sum over A+T (light blue), sum over AT + N (dark blue), and the difference (A+T) – (AT + N) (orange), i.e. the audiotactile interaction effects across different asynchrony levels, as well as unisensory and null conditions separately. We observed significant AT interactions for ITC in the theta band (4-8 Hz) specifically for ±70 ms asynchrony levels (Figure 4, AT70 and TA70 rows; Figure 2 for significance test results). As shown in Figure 4, the summed 'AT+N' ITC was greater than the summed 'A+T' for the auditory leading AT70, but smaller for tactile leading TA70 condition. Thus, the direction of the audiotactile ITC interaction depends on whether the auditory or the tactile sense is leading. The AT interaction arose at about 200 ms post-stimulus and was most prominent over frontocentral electrodes, mimicking the AT interactions we observed for the P200 in the ERP analysis (Figure 3B, AT70 and TA70 rows). In summary, the AT interactions for the theta-band ITC were selective for ±70 ms asynchronies and most likely associated with the ERP effects at the same post-stimulus latency and asynchrony conditions.

Audiotactile interactions for time-frequency power across AT asynchronies

Figure 5 shows the TF power for the sum over A+T (light blue), sum over AT + N (dark blue), and the difference (A+T) – (AT + N) (orange), i.e. the audiotactile interaction effects across different asynchrony levels, as well as unisensory and null conditions separately. For significance test results, see Figure 2.

Theta power: Both auditory and tactile stimuli induced theta power peaking at about 200 ms post-stimulus primarily over fronto-central electrodes (Figure 5; Unisensory row). This peak in theta power corresponds to the P200 (Figure 3) in the ERP analysis and an increase in ITC (Figure 4). Note that our data illustrate the point that the 'A+T' sum (Figure 5: AT0 light blue), which was computed by first summing trials before frequency transformation according to Senkowski et al. (2007), is indeed different than if the power of the tactile (Figure 5: Unisensory pink) and auditory (Figure 5: Unisensory green) had first been computed and then summed.

We observed significant AT interactions in the theta band at about 200 ms post-stimulus over fronto-central electrodes across several asynchrony levels including AT70, AT20, and TA70. These fronto-central AT interactions arose as a result of the AT+N power peak being weaker and decaying earlier relative to the A+T sum. Critically, these fronto-central AT interactions for theta power were most pronounced for ± 70 ms asynchrony levels, expressed less strongly for ± 20 ms and ± 500 ms asynchrony and completely absent for synchrony AT0 stimulation (see also Figure 6d).

In addition, we observed significant AT interactions for theta power in the AT500 condition. Specifically, in both early (60-600 ms) and late (610-1200 ms) time windows, AT interactions were found with topographies that were distinct from the fronto-central P200-like theta-band effects.

Alpha/Beta power: Because unisensory power changes and AT interactions were qualitatively similar between the alpha and the low-beta bands, we combined these into one alpha/beta band (8-20 Hz). Both tactile and auditory stimuli induced changes in the alpha/beta band primarily over posterior channels (Figure 5, Unisensory row), which were more pronounced for tactile stimulation. Auditory and tactile stimulation initially suppressed alpha/beta power (event-related desynchronization; ERD) around 250 ms post-stimulation followed by a rebound (event-related synchronisation; ERS) above and beyond baseline, around 800-1000 ms post-stimulation. This alpha/beta power rebound was altered for AT + N relative to A + T across several asynchrony levels including AT70, AT20, AT0, and TA70 conditions (Figure 2 for statistics and Figure 5). Specifically, the rebound in alpha/beta power occurred earlier, was attenuated, and decayed faster for AT+N than the A+T sum, where alpha/beta power rebound was found to be more sustained (800-1100 ms post-stimulation).

Summary of AT integration effects

To provide an overview over the diverse AT interactions that we observed for ERPs, ITC, and TF power, Figure 6 summarises the results, averaged over relevant spatial, temporal, and frequency selections: the sum of the auditory and tactile (A+T; light blue), the sum of audiotactile plus null (AT+N; dark blue) and the audiotactile interaction, i.e. the difference [AT+N]-[A+V] as a function of AT asynchrony: 0, ±20, ±70, ±500 ms. This enables us to characterise the profile of the AT interaction effects across asynchrony levels, including sub-threshold effects in one asynchrony that relate to a significant effect in another asynchrony.

386 The early (~125 ms latency) AT interactions for ERPs followed an inverted U-shape function
387 that was constrained by a ≤20 ms TIW. They were significant only for AT0 and tapered off with
388 subthreshold effects at AT20 (Figure 6a).

389 The AT interactions for P200 in ERPs and theta band ITC at ~200 ms were significant
390 selectively for ± 70 ms AT asynchronies (Figure 6b and 6c). Surprisingly, the interactions for the
391 ERPs (i.e. P200) were symmetric and positive for both auditory and tactile leading asynchrony,
392 while the interactions for the ITC were asymmetric, i.e. negative for A leading and positive for T
393 leading asynchrony levels. This asymmetry and asynchrony specificity indicates that these ITC
394 effects are sensitive to the relative timing of the auditory and tactile signals - pointing towards
395 mechanisms of phase resetting.

396 The corresponding AT interactions for theta band TFP at ~200 ms post-stimulus were present
397 (at least at a sub-threshold level) across all AT asynchronies except for the physically
398 synchronous AT stimulation (Figure 6d). Specifically, we observed significant AT interactions
399 (i.e. reduction for AT+N relative to A+T) for AT500, AT70, AT20, and TA70 and non-
400 significant trends for TA20 and TA500.

401 The late AT interactions at ~400 ms latency for ERPs followed an inverted U-shape function
402 mimicking the response facilitation at the behavioural level (Figure 6e). These interactions were
403 significant for AT20 and TA20, with subthreshold effects for AT0, AT70, and TA70. Figure 3
404 shows that this late AT interaction emerges because the phase of the summed A+T response
405 ('trough') is in opposition to the phase of the summed AT+N response ('peak').

406 Finally, the late AT interactions for the alpha/beta band power "rebound" were observed
407 across several asynchronies (AT70, AT20, AT0, and TA70) (Figure 6f). They resulted from an

earlier occurrence and faster decay of the alpha/beta rebound for the AT+N compared to the sum A + T and were most pronounced for A leading asynchronies (Figure 5).

To summarise, AT interactions were expressed across AT asynchrony levels with three distinct profiles: i. inverted U-shape profile: early N100 and late 400 ms ERP effects, ii. most pronounced for AT asynchronies of ±70 ms: ERP, ITC theta, and TFP theta effects at about 200 ms, and iii. most prominent for A leading asynchronies and present even outside the behavioural TIW: late alpha/beta TFP rebound effects.

Discussion

The current study presented A, T, and AT stimuli at several asynchrony levels to investigate the temporal constraints that govern behavioural response facilitation and neural AT interactions for ERPs, ITC, and induced TF power.

Consistent with previous research (Colonius and Diederich, 2004), we observed an inverted U-shape function for the behavioural AT benefit – also coined the redundant target effect (Miller, 1982)- that was maximal for synchronous AT combinations and tapered off with increasing AT asynchrony within a TIW of ≤70 ms (Zampini et al., 2005).

At the neural level we observed early AT interactions for evoked responses (ERP) at about 110 ms post-stimulus, which dovetails nicely with previous research showing multisensory modulations of the N1 auditory component by visual and tactile stimuli (Foxe et al., 2000, Lutkenhoner et al., 2002, Murray et al., 2005, Sperdin et al., 2009, Stekelenburg and Vroomen, 2009). Critically, our observed early AT interactions were sensitive to the relative timing of the AT stimuli: they were most pronounced for synchronous AT stimuli and tapered off within a small TIW of ≤20 ms. This temporal precision may be enhanced for interactions of tactile with

other sensory signals, because tactile latencies are fixed for a particular body location and do not vary depending on the distance of the stimulus from the observer as in audition and vision. The short latency and narrow temporal binding window points towards neural interactions in low level or even primary auditory cortices that may rely on direct connectivity between sensory areas (Fu et al., 2003, Cappe and Barone, 2005, de la Mothe et al., 2006a, Smiley et al., 2007) or thalamic mechanisms (de la Mothe et al., 2006b, Hackett et al., 2007, Cappe et al., 2009) and that increase the saliency of AT events leading to faster and more accurate detection.

Later, at about 400 ms post-stimulus, we observed audiotactile ERP interactions that were again most pronounced for synchronous AT stimuli, but confined to a broader TIW of ≤70 ms, which is consistent with a hierarchical organisation of AT interactions where early effects in low level sensory areas are confined to a narrower temporal integration windows than later interactions in association cortices (Hasson et al., 2008, Kiebel et al., 2008, Werner and Noppeney, 2011). Moreover, the later interactions may in turn top-down modulate neural processes in lower regions via feed-back loops (Falchier et al., 2002, Schroeder and Foxe, 2002, Clavagnier et al., 2004). Both early and late ERP interactions followed an inverted U-shape function thereby mimicking the temporal profile of the redundant target effect that characterised observers' behaviour.

While the ERP effects at ~125 ms and ~400 ms post-stimulus were constrained by classical temporal integration windows, the AT interactions for the P200 ERP component were most pronounced for ± 70 ms AT asynchrony and absent for near-synchronous AT stimulation (see Figure 3 and Figure 6b). Both the auditory and the tactile unisensory P200 are thought to be generated in regions previously implicated in audiotactile integration (Foxe et al., 2002, Kayser et al., 2005, Murray et al., 2005, Schurmann et al., 2006) such as the auditory belt area CM or

454 planum temporale (Godey et al., 2001, Crowley and Colrain, 2004, Smiley et al., 2007) and
455 secondary somatosensory areas (Forss et al., 1994, Disbrow et al., 2001), respectively. Our
456 results show that AT integration facilitates neural processing at about 200 ms post-stimulus: the
457 P200 peaks earlier, is smaller, and/or decays faster for the AT+N sum when compared to the sum
458 of the unisensory A and T conditions, consistent with multisensory literature, e.g. (Rowland et
459 al., 2007).

460 The P200 effects were also directly related to AT interactions for theta-band ITC that
461 emerged with a central topography again at ~200 ms post-stimulus selectively for ± 70 ms AT
462 asynchrony (compare Figures 6b and 6c). Critically, whilst the ERP interactions followed a
463 similar temporal profile and topography irrespective of whether the auditory or the tactile
464 stimulus is leading, the ITC effects were inverted for auditory relative to tactile leading
465 stimulation. This dissociation between ERP and ITC can be shown to occur in simulation
466 (https://github.com/johanna-zumer/audtac/blob/master/simulate_70results.m). The selectivity of
467 the P200 and the phase coherence effects for ± 70 ms AT asynchrony may be best accounted for
468 by mechanisms of phase resetting that have previously been implicated in audiotactile and
469 audiovisual interactions in auditory cortices (Lakatos et al., 2007, Kayser et al., 2008, Thorne et
470 al., 2011). From a functional perspective, a preceding tactile stimulus may reset the phase in
471 auditory cortices and thereby facilitate the localization of an auditory stimulus that is presented
472 70 ms later. Likewise, a preceding auditory stimulus may provide an alert to facilitate tactile
473 processing and possible avoidance actions. Not only have tones been shown to elicit responses
474 in somatosensory cortex (Borgest and Ermolaeva, 1975, Liang et al., 2013), but also an
475 *inhibitory* multisensory interaction by auditory stimulation was found in cat somatosensory area
476 SIV (Dehner et al., 2004) and auditory projections were found to inhibitory interneurons in cat

SIV (Keniston et al., 2010). In summary, our P200 and ITC results are supported by evidence of bidirectional audiotactile integration, especially to association cortices, and of directional asymmetries in the AT interaction (Cecere et al., 2017).

The AT interactions discussed so far were moulded by two distinct neural mechanisms: i. ERP effects at ~100 and ~400 ms that followed an inverted U-shape function mimicking the temporal binding window at the behavioural level and ii. P200 and theta ITC effects that were selective for a particular level of AT asynchrony and may be mediated by mechanisms of phase resetting. In contrast, AT interactions for induced theta oscillatory power were less specific and expressed not only for ± 70 ms asynchrony, but across several asynchrony levels in particular when the auditory stimulus was leading. While the topography and timing of the theta TF power interactions *within* the TIW matched that of the P200 and ITC interactions, a distinct topographical effect was found *outside* the classical behavioural integration window, in the AT500 condition. Further, this enhanced oscillatory theta power was sustained until 1150 ms, i.e. beyond the time needed to make a response in the redundant target paradigm of the associated psychophysics study. We suggest that the AT theta power effects may reflect non-specific mechanisms of multisensory priming or attention by which a preceding A signal may alert the observer to imminent touch events, in light of the debate as to whether cross-modal stimuli with asynchronies up to 500-600 ms may be actually *integrated* or whether the first stimulus (only) primes and/or draws exogenous (spatial) cross-modal attention (Macaluso et al., 2001, McDonald et al., 2001, Stein et al., 2010). Alternatively, the AT500 condition may be viewed as a type of “No-go” trial in which a response to the second stimulus is to be withheld, which has previously been shown to be associated with frontal theta oscillations (Kirmizi-Alsan et al., 2006, Harper et al., 2014).

Likewise, we observed AT interactions for alpha/beta oscillatory power at ~1000 ms post-stimulus. As shown in Figure 5, both auditory and tactile stimuli suppressed alpha/beta oscillatory power (event-related desynchronization; ERD) at about 200-400 ms, related to a release from inhibition, followed by a rebound in power beyond baseline levels from about 600 ms – 1200 ms post-stimulus (event-related synchronisation; ERS), related to resetting and recovery (Pfurtscheller and Lopes da Silva, 1999, Neuper and Pfurtscheller, 2001). Our results show that the initial suppression (ERD) of alpha/beta power is not significantly different from the sum of the auditory and tactile induced suppressions; yet, the rebound in alpha/beta power for the AT+Null sum is weaker and decays faster than predicted by the A+T sum of the additive model. Further, we observed significant AT interactions for the alpha/beta rebound for AT70, AT20, AT0, and TA70, and as a non-significant trend for the AT500 asynchrony level. Because the AT interactions of power rebound occurred after the explicit detection response is made by participants in the redundant target paradigm, it may be a consequence of the implicit AT event detection, or be associated with post-decisional processes such as metacognitive monitoring (Deroy et al., 2016), or the binding of asynchronous signals into a single multisensory percept (Roa Romero et al., 2015). Future redundant target paradigms that combine target detection with post-decisional tasks (e.g. confidence judgments) may enable us to further determine the functional role of the alpha/beta rebound and the associated AT interactions. The distinct response profile for theta versus alpha/beta power, varying with stimulus asynchrony, is in line with distinct mechanisms for different frequencies (Keil and Senkowski, 2018).

To conclude, this psychophysics-EEG study unravels a multitude of neural interactions, which arose with different temporal constraints: interactions were confined to a TIW for ERPs, specific for one particular asynchrony for inter-trial coherence, and extending beyond the behavioural

TIW for induced low frequency power. This diversity of temporal profiles demonstrates that distinct neural mechanisms govern a cascade of multisensory integration processes.

References:

Atilgan H, Town SM, Wood KC, Jones GP, Maddox RK, Lee AKC, Bizley JK (2018) Integration of Visual Information in Auditory Cortex Promotes Auditory Scene Analysis through Multisensory Binding. Neuron 97:640-655 e644.

Berger CC, Ehrsson HH (2014) The fusion of mental imagery and sensation in the temporal association cortex. J Neurosci 34:13684-13692.

Bizley JK, Nodal FR, Bajo VM, Nelken I, King AJ (2007) Physiological and anatomical evidence for multisensory interactions in auditory cortex. Cereb Cortex 17:2172-2189.

Blurton SP, Greenlee MW, Gondan M (2015) Cross-modal cueing in audiovisual spatial attention. Atten Percept Psychophys 77:2356-2376.

Borgest AN, Ermolaeva V (1975) [Functional organization of pathways transmitting auditory signals in the somatosensory zone of the cat cerebral cortex]. Neirofiziologiia 7:476-485.

Cappe C, Barone P (2005) Heteromodal connections supporting multisensory integration at low levels of cortical processing in the monkey. Eur J Neurosci 22:2886-2902.

Cappe C, Morel A, Barone P, Rouiller EM (2009) The thalamocortical projection systems in primate: an anatomical support for multisensory and sensorimotor interplay. Cereb Cortex 19:2025-2037.

Cecere R, Gross J, Willis A, Thut G (2017) Being First Matters: Topographical Representational Similarity Analysis of ERP Signals Reveals Separate Networks for Audiovisual Temporal Binding Depending on the Leading Sense. J Neurosci 37:5274-5287.

546 Clavagnier S, Falchier A, Kennedy H (2004) Long-distance feedback projections to area V1:
547 implications for multisensory integration, spatial awareness, and visual consciousness.
548 Cogn Affect Behav Neurosci 4:117-126.
549 Colonius H, Diederich A (2004) Multisensory interaction in saccadic reaction time: a time-
550 window-of-integration model. J Cogn Neurosci 16:1000-1009.
551 Crowley KE, Colrain IM (2004) A review of the evidence for P2 being an independent
552 component process: age, sleep and modality. Clin Neurophysiol 115:732-744.
553 Dahl CD, Logothetis NK, Kayser C (2009) Spatial organization of multisensory responses in
554 temporal association cortex. J Neurosci 29:11924-11932.
555 de la Mothe LA, Blumell S, Kajikawa Y, Hackett TA (2006a) Cortical connections of the
556 auditory cortex in marmoset monkeys: core and medial belt regions. J Comp Neurol
557 496:27-71.
558 de la Mothe LA, Blumell S, Kajikawa Y, Hackett TA (2006b) Thalamic connections of the
559 auditory cortex in marmoset monkeys: core and medial belt regions. J Comp Neurol
560 496:72-96.
561 Dehner LR, Keniston LP, Clemo HR, Meredith MA (2004) Cross-modal circuitry between
562 auditory and somatosensory areas of the cat anterior ectosylvian sulcal cortex: a 'new'
563 inhibitory form of multisensory convergence. Cereb Cortex 14:387-403.
564 Deroy O, Spence C, Noppeney U (2016) Metacognition in Multisensory Perception. Trends
565 Cogn Sci 20:736-747.
566 Diederich A, Colonius H (2004) Bimodal and trimodal multisensory enhancement: effects of
567 stimulus onset and intensity on reaction time. Percept Psychophys 66:1388-1404.

568 Disbrow E, Roberts T, Poeppel D, Krubitzer L (2001) Evidence for interhemispheric processing
569 of inputs from the hands in human S2 and PV. J Neurophysiol 85:2236-2244.
570 Donohue SE, Green JJ, Woldorff MG (2015) The effects of attention on the temporal integration
571 of multisensory stimuli. Front Integr Neurosci 9:32.
572 Downar J, Crawley AP, Mikulis DJ, Davis KD (2000) A multimodal cortical network for the
573 detection of changes in the sensory environment. Nat Neurosci 3:277-283.
574 Falchier A, Clavagnier S, Barone P, Kennedy H (2002) Anatomical evidence of multimodal
575 integration in primate striate cortex. J Neurosci 22:5749-5759.
576 Fetsch CR, Pouget A, DeAngelis GC, Angelaki DE (2011) Neural correlates of reliability-based
577 cue weighting during multisensory integration. Nat Neurosci 15:146-154.
578 Forss N, Salmelin R, Hari R (1994) Comparison of somatosensory evoked fields to airpuff and
579 electric stimuli. Electroencephalogr Clin Neurophysiol 92:510-517.
580 Foxe JJ, Morocz IA, Murray MM, Higgins BA, Javitt DC, Schroeder CE (2000) Multisensory
581 auditory-somatosensory interactions in early cortical processing revealed by high-density
582 electrical mapping. Brain Res Cogn Brain Res 10:77-83.
583 Foxe JJ, Schroeder CE (2005) The case for feedforward multisensory convergence during early
584 cortical processing. Neuroreport 16:419-423.
585 Foxe JJ, Wylie GR, Martinez A, Schroeder CE, Javitt DC, Guilfoyle D, Ritter W, Murray MM
586 (2002) Auditory-somatosensory multisensory processing in auditory association cortex:
587 an fMRI study. J Neurophysiol 88:540-543.
588 Fu KM, Johnston TA, Shah AS, Arnold L, Smiley J, Hackett TA, Garraghty PE, Schroeder CE
589 (2003) Auditory cortical neurons respond to somatosensory stimulation. J Neurosci
590 23:7510-7515.

591 Ghazanfar AA, Schroeder CE (2006) Is neocortex essentially multisensory? Trends Cogn Sci
592 10:278-285.
593 Giard MH, Peronnet F (1999) Auditory-visual integration during multimodal object recognition
594 in humans: a behavioral and electrophysiological study. J Cogn Neurosci 11:473-490.
595 Godey B, Schwartz D, de Graaf JB, Chauvel P, Liegeois-Chauvel C (2001) Neuromagnetic
596 source localization of auditory evoked fields and intracerebral evoked potentials: a
597 comparison of data in the same patients. Clin Neurophysiol 112:1850-1859.
598 Hackett TA, De La Mothe LA, Ulbert I, Karmos G, Smiley J, Schroeder CE (2007) Multisensory
599 convergence in auditory cortex, II. Thalamocortical connections of the caudal superior
600 temporal plane. J Comp Neurol 502:924-952.
601 Harper J, Malone SM, Bernat EM (2014) Theta and delta band activity explain N2 and P3 ERP
602 component activity in a go/no-go task. Clin Neurophysiol 125:124-132.
603 Harrar V, Harris LR (2008) The effect of exposure to asynchronous audio, visual, and tactile
604 stimulus combinations on the perception of simultaneity. Exp Brain Res 186:517-524.
605 Hasson U, Yang E, Vallines I, Heeger DJ, Rubin N (2008) A hierarchy of temporal receptive
606 windows in human cortex. J Neurosci 28:2539-2550.
607 Hershenson M (1962) Reaction time as a measure of intersensory facilitation. J Exp Psychol
608 63:289-293.
609 Hoefer M, Tyll S, Kanowski M, Brosch M, Schoenfeld MA, Heinze HJ, Noesselt T (2013)
610 Tactile stimulation and hemispheric asymmetries modulate auditory perception and
611 neural responses in primary auditory cortex. Neuroimage 79:371-382.

612 Ibrahim LA, Mesik L, Ji XY, Fang Q, Li HF, Li YT, Zingg B, Zhang LI, Tao HW (2016) Cross-
613 Modality Sharpening of Visual Cortical Processing through Layer-1-Mediated Inhibition
614 and Disinhibition. Neuron 89:1031-1045.
615 Kayser C, Petkov CI, Augath M, Logothetis NK (2005) Integration of touch and sound in
616 auditory cortex. Neuron 48:373-384.
617 Kayser C, Petkov CI, Augath M, Logothetis NK (2007) Functional imaging reveals visual
618 modulation of specific fields in auditory cortex. J Neurosci 27:1824-1835.
619 Kayser C, Petkov CI, Logothetis NK (2008) Visual modulation of neurons in auditory cortex.
620 Cereb Cortex 18:1560-1574.
621 Keil J, Senkowski D (2018) Neural Oscillations Orchestrate Multisensory Processing.
622 Neuroscientist 1073858418755352.
623 Keniston LP, Henderson SC, Meredith MA (2010) Neuroanatomical identification of crossmodal
624 auditory inputs to interneurons in somatosensory cortex. Exp Brain Res 202:725-731.
625 Kiebel SJ, Daunizeau J, Friston KJ (2008) A hierarchy of time-scales and the brain. PLoS
626 Comput Biol 4:e1000209.
627 Kirmizi-Alsan E, Bayraktaroglu Z, Gurvit H, Keskin YH, Emre M, Demiralp T (2006)
628 Comparative analysis of event-related potentials during Go/NoGo and CPT:
629 decomposition of electrophysiological markers of response inhibition and sustained
630 attention. Brain Res 1104:114-128.
631 Lakatos P, Chen CM, O'Connell MN, Mills A, Schroeder CE (2007) Neuronal oscillations and
632 multisensory interaction in primary auditory cortex. Neuron 53:279-292.
633 Leclercq Y, Schrouff J, Noirhomme Q, Maquet P, Phillips C (2011) fMRI artefact rejection and
634 sleep scoring toolbox. Comput Intell Neurosci 2011:598206.

635 Leonardelli E, Braun C, Weisz N, Lithari C, Occelli V, Zampini M (2015) Prestimulus
636 oscillatory alpha power and connectivity patterns predispose perceptual integration of an
637 audio and a tactile stimulus. Hum Brain Mapp 36:3486-3498.
638 Liang M, Mouraux A, Hu L, Iannetti GD (2013) Primary sensory cortices contain distinguishable
639 spatial patterns of activity for each sense. Nat Commun 4:1979.
640 Lutkenhoner B, Lammertmann C, Simoes C, Hari R (2002) Magnetoencephalographic correlates
641 of audiotactile interaction. Neuroimage 15:509-522.
642 Macaluso E, Frith C, Driver J (2001) (Response to) Multisensory Integration and Crossmodal
643 Attention Effects in the Human Brain. Science 292:1791-1791.
644 McDonald JJ, Teder-Sälejärvi WA, Ward LM (2001) Multisensory Integration and Crossmodal
645 Attention Effects in the Human Brain. Science 292:1791-1791.
646 Megevand P, Molholm S, Nayak A, Foxe JJ (2013) Recalibration of the multisensory temporal
647 window of integration results from changing task demands. PLoS One 8:e71608.
648 Mercier MR, Foxe JJ, Fiebelkorn IC, Butler JS, Schwartz TH, Molholm S (2013) Auditory-
649 driven phase reset in visual cortex: human electrocorticography reveals mechanisms of
650 early multisensory integration. Neuroimage 79:19-29.
651 Mercier MR, Molholm S, Fiebelkorn IC, Butler JS, Schwartz TH, Foxe JJ (2015) Neuro-
652 oscillatory phase alignment drives speeded multisensory response times: an electro-
653 corticographic investigation. J Neurosci 35:8546-8557.
654 Meredith MA, Stein BE (1983) Interactions among converging sensory inputs in the superior
655 colliculus. Science 221:389-391.
656 Miller J (1982) Divided attention: evidence for coactivation with redundant signals. Cogn
657 Psychol 14:247-279.

658 Molholm S, Ritter W, Murray MM, Javitt DC, Schroeder CE, Foxe JJ (2002) Multisensory
659 auditory-visual interactions during early sensory processing in humans: a high-density
660 electrical mapping study. Brain Res Cogn Brain Res 14:115-128.
661 Murray MM, Molholm S, Michel CM, Heslenfeld DJ, Ritter W, Javitt DC, Schroeder CE, Foxe
662 JJ (2005) Grabbing your ear: rapid auditory-somatosensory multisensory interactions in
663 low-level sensory cortices are not constrained by stimulus alignment. Cereb Cortex
664 15:963-974.
665 Navarra J, Soto-Faraco S, Spence C (2007) Adaptation to audiotactile asynchrony. Neurosci Lett
666 413:72-76.
667 Neuper C, Pfurtscheller G (2001) Event-related dynamics of cortical rhythms: frequency-specific
668 features and functional correlates. Int J Psychophysiol 43:41-58.
669 Nishi A, Yokoyama M, Ogawa K, Ogata T, Nozawa T, Miyake Y (2014) Effects of Voluntary
670 Movements on Audio-Tactile Temporal Order Judgment. Ieice T Inf Syst E97d:1567-
671 1573.
672 Oostenveld R, Fries P, Maris E, Schoffelen JM (2011) FieldTrip: Open source software for
673 advanced analysis of MEG, EEG, and invasive electrophysiological data. Comput Intell
674 Neurosci 2011:156869.
675 Pfurtscheller G, Lopes da Silva FH (1999) Event-related EEG/MEG synchronization and
676 desynchronization: basic principles. Clin Neurophysiol 110:1842-1857.
677 Roa Romero Y, Senkowski D, Keil J (2015) Early and late beta-band power reflect audiovisual
678 perception in the McGurk illusion. J Neurophysiol 113:2342-2350.
679 Rohe T, Noppeney U (2015) Cortical hierarchies perform Bayesian causal inference in
680 multisensory perception. PLoS Biol 13:e1002073.

681 Rohe T, Noppeney U (2016) Distinct Computational Principles Govern Multisensory Integration
682 in Primary Sensory and Association Cortices. Curr Biol 26:509-514.
683 Rowland BA, Quessy S, Stanford TR, Stein BE (2007) Multisensory integration shortens
684 physiological response latencies. J Neurosci 27:5879-5884.
685 Rowland BA, Stein BE (2007) Multisensory integration produces an initial response
686 enhancement. Front Integr Neurosci 1:4.
687 Schroeder CE, Foxe JJ (2002) The timing and laminar profile of converging inputs to
688 multisensory areas of the macaque neocortex. Brain Res Cogn Brain Res 14:187-198.
689 Schurmann M, Caetano G, Hlushchuk Y, Jousmaki V, Hari R (2006) Touch activates human
690 auditory cortex. Neuroimage 30:1325-1331.
691 Senkowski D, Gomez-Ramirez M, Lakatos P, Wylie GR, Molholm S, Schroeder CE, Foxe JJ
692 (2007) Multisensory processing and oscillatory activity: analyzing non-linear
693 electrophysiological measures in humans and simians. Exp Brain Res 177:184-195.
694 Senkowski D, Schneider TR, Foxe JJ, Engel AK (2008) Crossmodal binding through neural
695 coherence: implications for multisensory processing. Trends Neurosci 31:401-409.
696 Smiley JF, Hackett TA, Ulbert I, Karmas G, Lakatos P, Javitt DC, Schroeder CE (2007)
697 Multisensory convergence in auditory cortex, I. Cortical connections of the caudal
698 superior temporal plane in macaque monkeys. J Comp Neurol 502:894-923.
699 Sperdin HF, Cappe C, Foxe JJ, Murray MM (2009) Early, low-level auditory-somatosensory
700 multisensory interactions impact reaction time speed. Front Integr Neurosci 3:2.
701 Stanford TR, Quessy S, Stein BE (2005) Evaluating the operations underlying multisensory
702 integration in the cat superior colliculus. J Neurosci 25:6499-6508.

703 Stein BE, Burr D, Constantinidis C, Laurienti PJ, Alex Meredith M, Perrault TJ, Jr.,
704 Ramachandran R, Roder B, Rowland BA, Sathian K, Schroeder CE, Shams L, Stanford
705 TR, Wallace MT, Yu L, Lewkowicz DJ (2010) Semantic confusion regarding the
706 development of multisensory integration: a practical solution. Eur J Neurosci 31:1713-
707 1720.
708 Stekelenburg JJ, Vroomen J (2009) Neural correlates of audiovisual motion capture. Exp Brain
709 Res 198:383-390.
710 Thorne JD, De Vos M, Viola FC, Debener S (2011) Cross-modal phase reset predicts auditory
711 task performance in humans. J Neurosci 31:3853-3861.
712 van Wassenhove V, Grant KW, Poeppel D (2007) Temporal window of integration in auditory-
713 visual speech perception. Neuropsychologia 45:598-607.
714 Werner S, Noppeney U (2010a) Distinct functional contributions of primary sensory and
715 association areas to audiovisual integration in object categorization. J Neurosci 30:2662-
716 2675.
717 Werner S, Noppeney U (2010b) Superadditive responses in superior temporal sulcus predict
718 audiovisual benefits in object categorization. Cereb Cortex 20:1829-1842.
719 Werner S, Noppeney U (2011) The contributions of transient and sustained response codes to
720 audiovisual integration. Cereb Cortex 21:920-931.
721 Zampini M, Brown T, Shore DI, Maravita A, Roder B, Spence C (2005) Audiotactile temporal
722 order judgments. Acta Psychol (Amst) 118:277-291.

723

724

Legends

Figure 1. Experimental design, behavioural results, and evoked responses. ***a,*** Each row depicts the onsets of the auditory stimulation (indicated by loudspeaker) and tactile stimulation (indicated by face) for each of the 10 conditions including the null (N), auditory alone (A), tactile alone (T) and the seven AT conditions with asynchrony: 0, ±20, ±70, and ±500 ms. The wavy line at the bottom indicates the continuous MRI background noise. ***b,*** Reaction times (across subjects' mean ± SEM). The black lines indicate the AT conditions as a function of AT asynchrony with negative asynchronies indicating auditory-leading; the green and pink bars indicate the A and T conditions, respectively. ***c,*** Evoked response potentials for N, A, T, and AT conditions for frontocentral ['Fz' 'Cz' 'F1' 'F2' 'FC1' 'FC2' 'C1' 'C2'] and posterior ['CP5' 'POz' 'Pz' 'P3' 'P4' 'C4' 'O1' 'O2' 'P7' 'PO7'] sets of sensors. The A evoked response is shifted by the appropriate asynchrony to align with the auditory onset in the corresponding AT condition.

Figure 2: Statistics for behavioural and neural results for each AT asynchrony (rows). *Behavioural redundant target effect (RTE)*: paired t-tests (sample size: N=22; degrees of freedom = 21) comparing the AT response time with the minimal unisensory response time. For AT500 the AT response was slower than the minimal unisensory response (negative t-value). The "e" indicates "x 10^". *Neural AT interactions* [(A+T) – (AT + N)] for ERPs (blue), ITC (violet), and TFP (red) listed in separate columns for different latency ranges: non-parametric permutation dependent/paired samples t-tests (sample size N=22) comparing A+T with AT+N. The p-values are reported at the cluster level (max sum) corrected for multiple comparisons over channels and time (and frequency for ITC and TFP) with an auxiliary uncorrected threshold of $p<0.05$. P-values in italics indicate a non-significant trend.

748

749 **Figure 3.** Evoked response potentials. Each row shows the audiotactile interaction for a
750 particular level of AT asynchrony. (A) ERPs of the sum of the auditory and tactile (A+T; light
751 blue), the sum of audiotactile plus null (AT+N; dark blue), and the audiotactile interaction, i.e.
752 the difference ([A+T]-[AT+N], orange). Green = auditory onset, pink = tactile onset. Shaded
753 grey areas indicate the timing of significant AT interactions at $p < 0.05$ corrected at the cluster
754 level for multiple comparisons across electrodes and time points within a 500 ms window
755 starting with the second stimulus and limited by the black dashed line. (B) Topographies of the
756 sums: A+T, AT+N, and (A+T)-(AT+N) for time windows of significant AT interactions. The
757 time windows written in orange are relative to the onset of the second stimulus. A black star over
758 an electrode indicates that it is part of a significant cluster.

759

760 **Figure 4.** Inter-trial coherence. Each row shows the audiotactile interaction in the ITC for a
761 particular level of AT asynchrony, plus the unisensory conditions. (A) ITC of the sum of the
762 auditory and tactile (A+T; light blue), the sum of audiotactile plus null (AT+N; dark blue), and
763 the audiotactile interaction, i.e. the difference ([A+T]-[AT+N], orange). The bottom row shows
764 the Null (grey), Tactile (pink), and Auditory (green) conditions. Green = auditory onset, pink =
765 tactile onset. Shaded grey areas indicate the timing of significant AT interactions at $p < 0.05$
766 corrected at the cluster level for multiple comparisons across electrodes, frequency, and time
767 points within a 1200 ms window starting with the second stimulus and limited by the black
768 dashed line. (B) Topographies of the sums: A+T, AT+N, and (A+T)-(AT+N) for time windows
769 of significant AT interactions. The time windows written in orange are relative to the onset of the
770 second stimulus. A black star over an electrode indicates that it is part of a significant cluster.

Figure 5. Time-frequency power. Each row shows the audiotactile interaction for a particular level of AT asynchrony. (A) Theta and (B) Alpha/Beta power of the sum of the auditory and tactile (A+T; light blue), the sum of audiotactile plus null (AT+N; dark blue), and the audiotactile interaction, i.e. the difference ([A+T]-[AT+N], orange). The bottom row shows the null (grey), tactile (pink), and auditory (green) condition. Green = auditory onset, pink = tactile onset. Shaded grey areas indicate the timing of significant AT interactions at $p < 0.05$ corrected at the cluster level for multiple comparisons across electrodes, frequency, and time points within a 1200 ms window starting with the second stimulus and limited by the black dashed line. (C) Topographies of the sums: A+T, AT+N, and (A+T)-(AT+N) for time windows of significant AT interactions, arranged in the same way as in Figures 3 and 4. The time windows written in orange are relative to the onset of the second stimulus. A black star over an electrode indicates that it is part of a significant cluster.

Figure 6: Summary of six audiotactile interactions (rows a-f) for ERP, ITC, and TFP across the seven asynchrony levels. *Left:* Topographies of ERP, ITC, or TFP (as indicated), centred around a post-stimulus time (as indicated ± 20 ms), for a particular AT asynchrony level (as indicated in orange). *Right*: Line plots showing ERP, ITC, or TFP of the sum of the auditory and tactile (A+T; light blue), the sum of audiotactile plus null (AT+N; dark blue), and the audiotactile interaction, i.e. the difference ([A+T]-[AT+N]; orange) as a function of AT asynchrony: 0, ±20, ±70, and ±500 ms. The values are averaged across the representative electrodes highlighted in the topographies (left) and within a 40 ms time window centred on the latencies specified alongside the corresponding topographies. For interpretational purposes, the labels ‘U’ and ‘70’

794 indicate via colour coding whether 'A+T' and 'AT+N' (blue) or the AT interaction (orange)

795 follow a U-shape function (= U) or are selective for ±70 ms asynchrony (= 70).

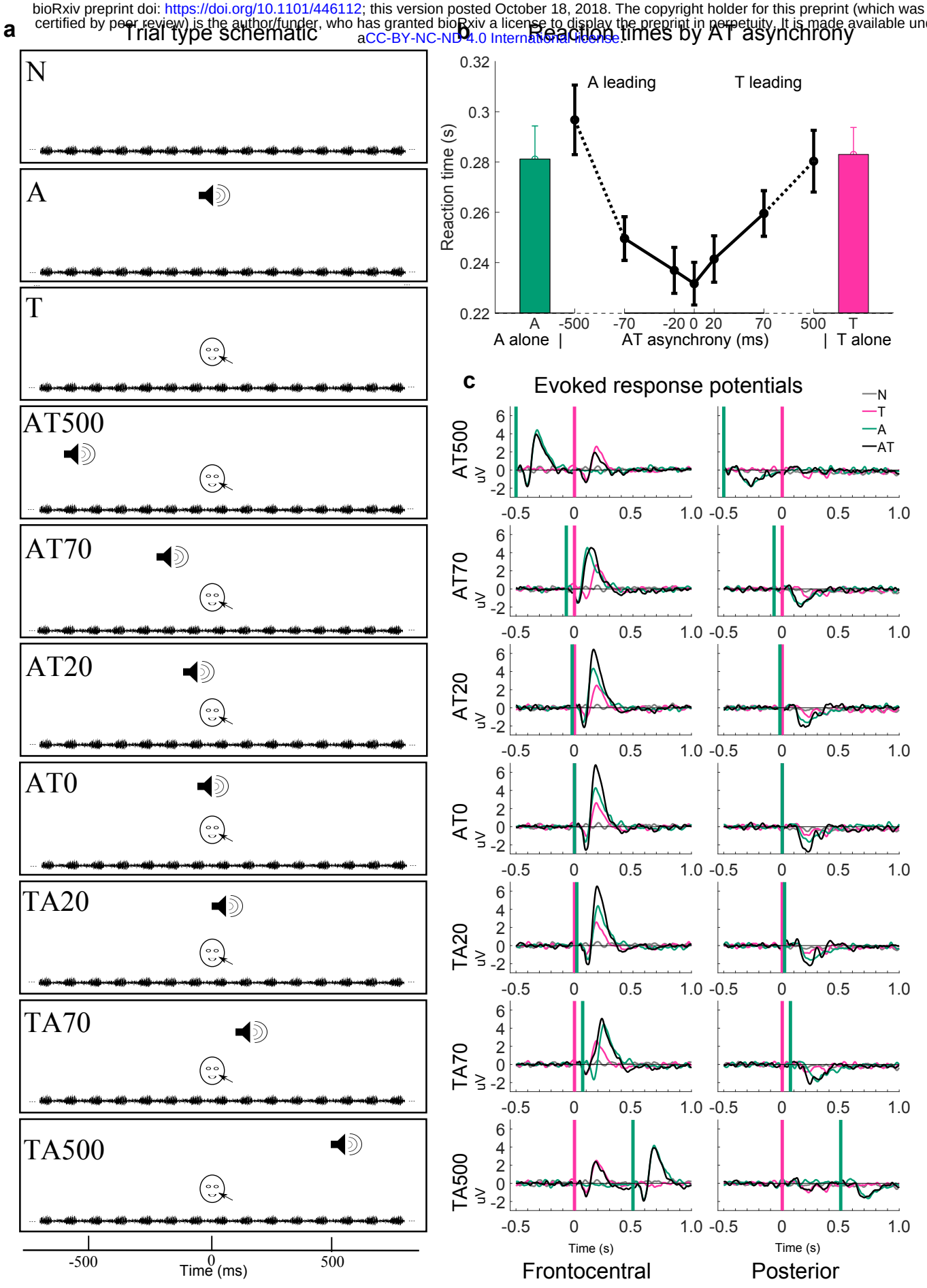

MSI effects	Behaviour:	Neural Post-stimulus Latency:			
Asynchrony:	RTE	~125 ms	~200 ms	~400 ms	~800-1100 ms
AT500	p=0.001 t=3.4				
AT70	p=1.2e-5 t=5.7		ERP 120-270 ms (p=0.010) θ ITC 0-260 ms (p=0.037) θ TFP 90-640 ms (p=0.01)		β TFP 1030-1150 ms (p=0.042)
AT20	p=7.2e-8 t=8.1	*ERP 40-100 ms (p=0.072)*	θ TFP 0-470 ms (p=0.049)	ERP 370-420 ms (p=0.022)	α & β TFP 700-1000 ms (p=0.027)
AT0	p=1.1e-7 t=7.8	ERP 70-170 ms (p=0.017)		*ERP 370-420 ms (p=0.28)*	α & β TFP 840-1140 ms (p=0.017)
TA20	p=2.1e-8 t=8.7			ERP 340-400 ms (p=0.03)	
TA70	p=8.8e-5 t=4.8		ERP 140-220 ms (p=0.007) θ ITC 0-490 ms (p=0.0005) θ TFP 0-480 ms (p=0.005)		α/β TFP 870-1200 ms (p=0.023)
TA500